The Properties of Polyimide Targets

In 1996 LLE began a research effort to make spherical capsules from polyimide material for use in direct-drive inertial confinement fusion (ICF) experiments. Previously, ICF capsules were made exclusively from glass, polystyrene, or an amorphous carbon–hydrogen solid solution referred to as "plasma polymer" or "glow-discharge polymer."[1] Polyimide was first proposed as a potential material for a target wall in 1995 because of its appreciable strength;[2] however, no viable method for making these capsules was identified. Following a five-year development project, a process for making polyimide capsules was developed and demonstrated, and the technology transferred to General Atomics—the ICF target fabricator—for production. As part of the project, polyimide shells with various properties relevant to ICF were developed. Those properties will be presented and compared in this article.

The fabrication method and associated properties of the different direct-drive polyimide targets have been reported previously.[3–5] This article summarizes and compares those properties that are important for producing cryogenic targets. Furthermore, issues that are unique to providing cryogenic targets, which impose stringent demands on performance from the shell material, are explained.

The properties of polyimide of importance to direct-drive ICF experiments are those that will increase the survivability of the shell during the process used to make cryogenic deuterium–tritium targets: specifically, the mechanical and permeation properties and the resistance of the material to embrittlement in a radioactive (tritium) environment. The rationale for choosing polyimide as a candidate material is that the polyimide chemical structure is one of the strongest polymeric materials, and among the most radiation resistant polymers,[6] and it should have the greatest likelihood of surviving demanding processing conditions.

Shells used for direct-drive ICF experiments need to be as robust as possible to withstand the inherent pressure gradients present when equipment has to operate over a wide pressure and temperature range. Shells are typically ~900 to 950 μm in diameter with the wall as thin as possible (1 to 3 μm) to minimize Raleigh–Taylor (RT) instabilities. The shell becomes an ICF target when it contains a nominal 100-μm layer of deuterium ice, which will include tritium in future experiments. The ice layer is achieved by first permeating gas at room temperature (or greater) into the shell and then cooling the shell and gas to below the triple point (for deuterium) at 18.73 K. The challenge in this process is caused by the fragility of the shell, which because of its large aspect ratio (diameter to wall thickness) can withstand only a very small pressure differential. This limits the driving force for permeation: it can take many days to fill the capsule with the sizeable gas inventory required to yield a 100-μm ice layer, and a well-controlled thermal environment is required to prevent the target from bursting or buckling.

During the permeation filling cycle, which can occur at temperatures from 270 to 500 K, and the subsequent cooling process to 18 K, the radioactive tritium gas decays with a half-life of 12.3 years and releases an electron with a mean energy of 6 keV. These high-energy electrons rupture chemical bonds, thereby weakening the capsule material. This creates a self-limiting cycle where increasingly long filling/cooling times de-rate the capsule's strength, which in turn requires even longer filling/cooling times. It has yet to be established that high-aspect-ratio shells can even be filled with tritium to the desired pressure without rupturing.

Finally, there is a requirement to minimize the processing time (filling and cooling cryogenic targets) as tritium decay produces a helium atom that will affect the convergence, and hence performance, of an imploding target. Given the tritium decay rate (0.015% conversion of T to ^{3}He per day), the desired duration for filling and cooling cryogenic targets is less than three days.

The sections that follow discuss (1) the mechanical properties of polyimide shells; (2) the techniques for changing the

shell's permeability by controlling the composition and microstructure of the polyimide; (3) the cooling of targets; and (4) the effects of radiation on shell properties.

The Structural Behavior and Properties of Polyimide Shells

1. The Mechanics of a Shell's Response to a Pressure Differential

A pressure differential across a shell's wall generates a uniform hydrostatic load within the wall that is resisted by in-plane forces (tension, compression, and shear) (see Fig. 92.18).[7] The magnitude of the induced forces can be analyzed solely by force-equilibrium equations (membrane theory) as long as the shell does not deform under the applied load, i.e., it is statically determined. Once the shell deforms, bending theory is needed to fully quantify the stress distribution in the shell and hence determine the maximum pressure differential a shell can withstand.
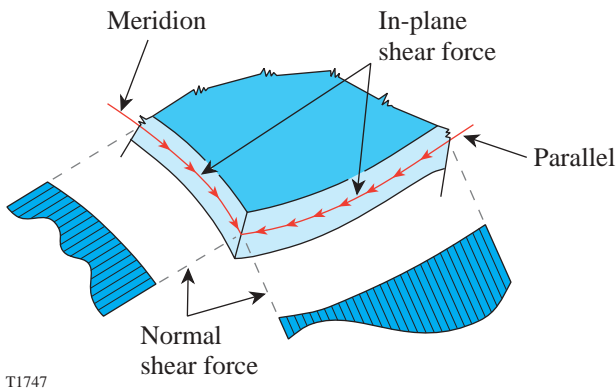

Figure 92.18
Schematic of the in-plane membrane forces present in a uniformly strained shell.

Direct-drive shells are classified as thin-walled shells; shells where the ratio of the wall thickness to the shell radius is less than 0.05 are categorized as "thin wall" and shells where the ratio is greater than 0.05 are "thick wall." This category of shell is unable to resist even small out-of-plane bending moments that easily deflect the wall. Once the shell is deformed, the intrinsic strength of the spherical geometry is compromised and the shell either shatters if it is brittle or collapses intact if it is elastic. Thicker-wall shells, such as indirect-drive shells, have a twofold strength advantage over thin-wall shells: first, the load-bearing capacity of the shell is greater, and second, once a shell begins to deflect to out-of-plane moments, the wall

more effectively resists the bending moment. Calculating the strength of thick-wall shells is also more complex since the bending theory is now an effective secondary reinforcement mechanism (membrane theory describes the primary mechanism) for resisting the applied load.

The buckle pressure is defined as that uniform load where the shell wall is at its maximum in-plane compression and shear stress, and any infinitesimal increase in pressure will cause the shell wall to deform. Increasing the pressure subjects the shell wall to bending moments, and at a critical pressure—the collapsing pressure—the shell collapses. The shells of interest in direct-drive ICF are all thin-wall (<5-μm) polymers with little resistance to out-of-plane forces, so the collapsing pressure is equal to the buckling pressure. The buckling pressure P_{buckle} is determined by the dimensions of the shell and the intrinsic properties of the material:[7]

$$P_{buckle} = \frac{2E}{\sqrt{3(1-v^2)}}\left(\frac{w}{r}\right)^2, \tag{1}$$

where E is the elastic modulus, σ is the tensile strength, v is Poisson's ratio (0.34), w is the wall thickness, and r is the radius.

The bursting pressure P_{burst} is analogous to the buckling pressure except that the internal pressure is greater than the external pressure and the in-plane forces are tensile (σ) and shear:

$$P_{burst} = 2\sigma(w/r). \tag{2}$$

ICF targets are not perfectly spherical, although the sphericity is excellent (0.5±0.2 μm out-of-round). This lack of sphericity decreases the buckling pressure from what would be expected for a perfectly spherical shell: At the region where the shell departs from perfect sphericity, the radius of curvature changes. Here the in-plane compressive stress acquires a shear component. This stress deflects the shell wall out-of-plane; the magnitude of the deflection and the affected area of the shell depend on the shear and flexural moduli, respectively. Thin-wall shells have little resistance to this out-of-plane force, so once the applied in-plane load can no longer be supported by in-plane compression, the strength of the spherical shape is compromised and the shell buckles. Shells where the radius of curvature changes abruptly, and that also have low shear and flexural moduli, will buckle at lower loads than rounder shells with greater stiffness.

Two phenomena combine to make thinner shells substantially more fragile: First, thinner-wall shells are more out-of-round than moderately thicker shell walls, a consequence of the shell fabrication process; second, as discussed above, thinner walls are inherently less resistant to bending moments than are moderately thicker shell walls. Experimentally it was observed that as the thickness of the shell wall decreases below $4\,\mu$m, the elastic modulus [Eq. (1)] becomes a weaker predictor of the maximum buckling pressure that a shell can withstand: There is a greater variation in the observed buckle pressure of a large sample of very thin wall shells (1 μm) compared to thicker shells. This behavior is not adequately explained by possible variations in the elastic modulus and Poisson ratios of different shells, which are intrinsic material properties independent of thickness; these properties depend upon the materials' microstructure, and supporting x-ray diffraction data show a similar microstructure for thick and thin films.[8,9] A more probable explanation for the greater variation in the buckle pressure of thin-wall shells is a greater variation in the roundness of the shells.

In the future, each shell will have to meet a specification for the maximum-allowable out-of-roundness to maximize the shell's survivability during processing. This will require the sphericity and uniformity of the wall thickness of each thin-wall shell to be quantified.

2. Fabrication of Thin-Wall Spherical Shells

Two effects can reduce the sphericity of the shell: First, there is the inherent out-of-roundness of the mandrel on which the polyimide shell is formed. Typically this value increases as the mandrel diameter increases. Second, a consequence of the polyimide-shell manufacturing is that additional out-of-roundness can be introduced during fabrication. Typically, this contribution is greater for thinner shell walls.[9]

The fabrication technique is summarized in Figs. 92.19 and 92.20. First, polyamic acid is deposited on a mandrel. The coated mandrel is then heated to convert polyamic acid into polyimide and simultaneously depolymerize the poly-α methyl-styrene mandrel. This depolymerization of the 30-μg mandrel would generate a burst pressure of 140 atm in the absence of permeation. Permeation does occur, however, and if the depolymerization rate is kept at or below the permeation rate, the polyimide shell will inflate only marginally and without exploding. Shells with walls as thin as 0.9 μm have been fabricated in this manner.[5,9] Shells can be made more out-of-round (beyond the limit established by the mandrel) during the depolymerization phase where expansion of the shell

stresses the plastic: If the shell material is strained beyond the yield point, it will plastically deform in those areas where the wall is thinnest. This nonuniform and nonrecoverable expansion will cause the shell to lose its sphericity when the internal pressure is reduced.[9]

While it is possible to make polyimide shells with the desirable strength and modulus properties, strict quality control will be required to select only the best geometries. Otherwise the greater mechanical properties of polyimide will not be realized.
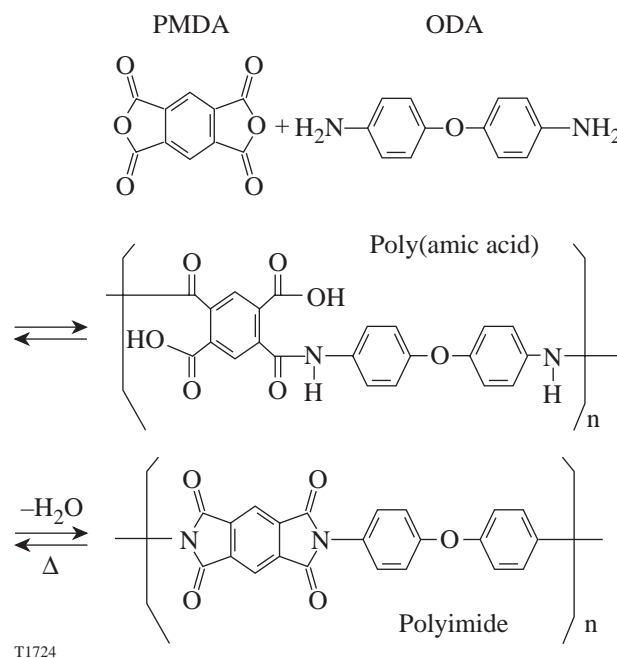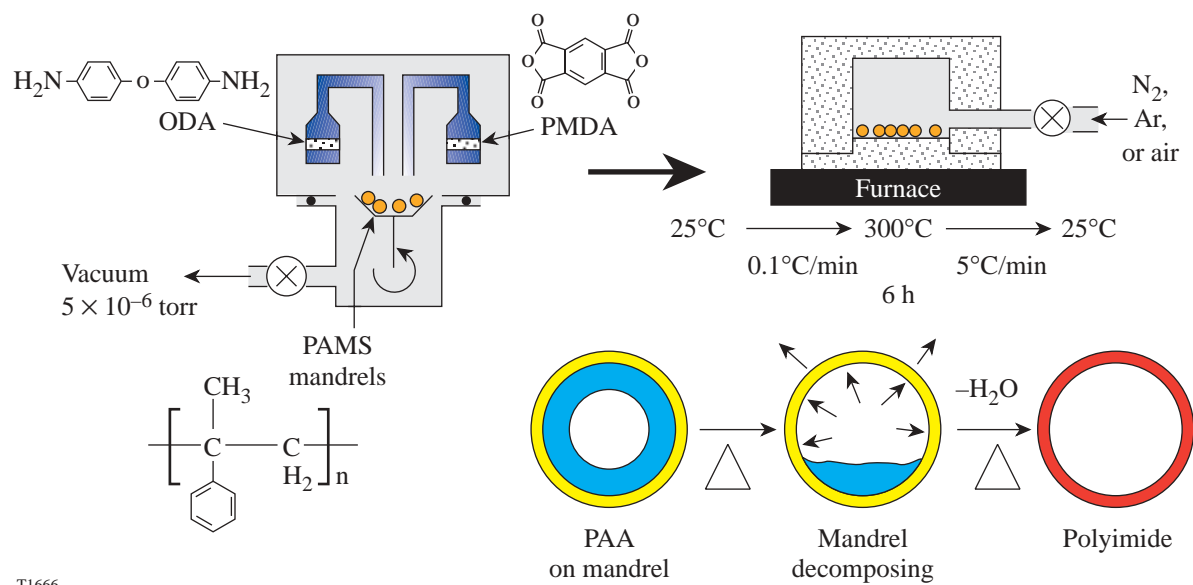

Figure 92.19
Schematic of the chemical process used to make polyimide shells using the vapor-deposition technique.

3. Stiffness, Strength, and Elasticity of Polyimide Shells

The physical properties of polyimide shells are listed in Table 92.I; the properties of plasma polymer shells are also listed for comparison. Generally, polyimide has greater physical properties than plasma polymer and, in addition, has a higher density, radiation resistance, and lower permeability, so the selection of one of these materials over the other as the optimal shell material is not immediately apparent. The implications of these other properties (permeability and radiation resistance) on the selection of polyimide or plasma polymer as a target material are expanded upon later.

T1666

Figure 92.20
Sequence of operations used to make polyimide shells.

The elastic modulus of vapor-deposited polyimide shells [calculated from Eq. (1)] was marginally larger than the literature-reported values for the same chemical formulation made using liquid processing: 3.2 GPa and 3.0 GPa, respectively.[10,11] There is a difference, however, in the method used to measure these values: using overpressure to buckle shells measures a biaxial compressive elastic modulus, whereas literature values for a commercial polyimide, Kapton™, are measured using American Standards and Testing Materials (ASTM) procedures with uniaxial tensile loading. The elastic modulus for vapor-deposited polyimide was also measured using an accepted nano-indentation method and was determined to be 4.0 GPa.[9]

The tensile strength of the polyimide was calculated from Eq. (2) by changing the pressure on either side of the shell and measuring the commensurate change in the diameter of the shell.[9,10] Vapor-deposited polyimide shells are appreciably stronger than solution-cast films, with ultimate strengths of 280±20 MPa and 170 MPa, respectively. The greater strength of the vapor-deposited polyimide material is attributed to the preferential alignment of the crystalline lattice in polyimide shells (discussed in detail later). Similar to the elastic-modulus measurements, pressure testing a shell to determine the tensile strength is a measure of the biaxial tensile stress–strain behav-

ior (in the plane of the shell), which is different from a uniaxial strength test of an ASTM-dimensioned measurement.

It is important to note that all testing of both polyimide and plasma polymer shells was to determine the optimal processing conditions as measured by each material's inherent stiffness, strength, and plasticity. No effort was intentionally made to preselect an underlying mandrel within a particular roundness and wall thickness specification. (This would have made the study too large, expensive, and intractable.) Therefore, the variation in the mandrels' sphericity is included in the statistical variation of the polyimide shells. This has the biggest effect on the reported elastic-modulus values of the shells, which are most susceptible to out-of-roundness effects. The possibility remains that future optimization and strict quality control of the underlying mandrels will improve the mechanical properties of both polyimide and plasma polymer shells.

The importance in ICF applications of having a higher-strength shell material is to improve the ability of the shell to (1) resist buckling pressures during permeation filling, (2) resist bursting and buckling pressures that develop within the permeation cell when a filled target is cooled to 20 K, and (3) resist bursting when the target is transferred (inside a cryostat) from the permeation cell to a cryostat.[12] This requires

Table 92.I: Comparison of the physical properties and chemical composition of available ICF shell materials.

Polymer Material	Elastic Modulus (GPa)	Ultimate Strength (MPa)	Elongation (%)	Chemical Composition	
				Atomic fraction (%)	
Polyimide (PMDA-ODA formulation) 1.42 gm/cm^3	3.2±0.1	280±12	27±2	C H N	56 26 5
Polyimide (6FDA-ODA formulations) 1.42 gm/cm^3	2.6±0.1	221±15	15±2	C H N O F	54 24 3 9 13
Plasma polymer[13] (high-density/ strength version) 1.18 gm/cm^3	2.7±0.2	88±10		C H	54 46
Plasma polymer[13] (baseline) 1.04 gm/cm^3	1.6±0.4	80±5		C H	43 57
Deuterated plasma polymer[13] (high-strength/ density version) 1.11 gm/cm^3	2.0±0.1	82±5		C D	61 39
Deuterated plasma polymer[13] 1.09 gm/cm^3	0.9±0.2			C D	59 41

that the elastic modulus and strength of the shell material be known over a wide temperature range (at least from 295 K to 18 K and more desirably from 573 K to 18 K to allow for higher-speed permeation at elevated temperatures). Typically, the room-temperature strength of the material is the most commonly reported value. The measured temperature dependences of the strength and elastic modulus are reported in Fig. 92.21. The elastic modulus is measured to increase by a factor of 2.5 over the temperature range 300 K to 130 K.

Polymers become stronger at lower temperatures, which increases the survivability of polymers in cryogenic applications. In ICF applications, however, use of only this value can be deceptive, since a plastically strained shell may have too high a permeability, which renders it useless, so the yield strength, below which a material behaves elastically, must also be known. Once a shell exceeds the yield strength, the change in the diameter in response to the applied stress is determined by the coefficient of hardening (the slope of the stress–strain curve in the plastic regime). This value is typically much smaller than the elastic modulus. A small stress in this regime can create a sizeable strain that will cause the shell to expand significantly and not recover its original dimensions. Moreover, the shell can deform (i.e., change in roundness) if the walls are not uniformly thick. By reason of this behavior the stress–strain relationship of the polyimide ideally should be known over the entire temperature range of interest (18 K to 573 K). This will allow the cryogenic target handling equipment to be designed to minimize the time required to provide ICF cryogenic targets (to limit the buildup of He^3). Obviously, equipment to handle cryogenic targets can be designed without detailed knowledge of the shell's behavior, but the design will

necessarily be conservative to ensure that the target survives processing, which is counter to the need to process targets as rapidly as possible.
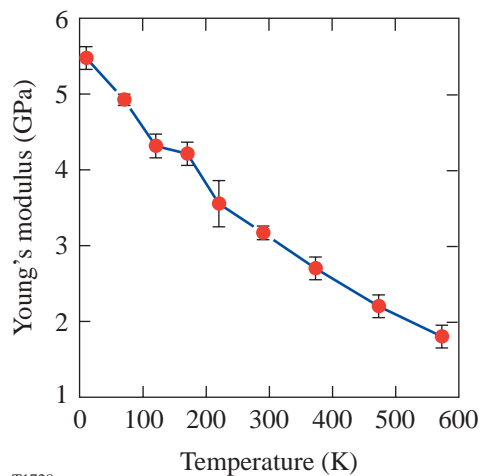
T1728

Figure 92.21
The temperature-dependent elastic modulus of polyimide from 12 K to 573 K.

4. Effects of Plastically Deforming Polyimide Shells

X-ray diffraction data of polyimide shells indicate the presence of a crystalline phase.[8] The crystal lattice plane is aligned perpendicular to the circumference of the shell as the polymer chain preferentially lies in the plane of the shell (see Fig. 92.22). This configuration gives the polyimide shell its strength and stiffness in compression/buckling, due to the stiffness of the lattice structure to out-of-plane forces, and also in tension/bursting, due to the alignment of the polymer backbone within the plane of the circumference.

When a polyimide shell is over-tensioned, as occurs when the internal pressure in the shell exceeds the yield stress of the material, the polyimide plastically deforms and the mechanical properties of the shell decrease: the buckle pressure decreases by 55%, which is attributed to the elastic modulus decreasing as the crystallinity of the material decreases,[9,10] and the shell becomes more nonspherical, which lowers the in-plane compressive and shear loads that the shell can withstand.

Of particular interest and relevance to ICF applications is the effect that plastically deforming polyimide has on the permeability of the material. A large sample of 120 polyimide shells were over-pressurized to determine the effect of strain on the permeability of the material to deuterium. The effect fell into one of two categories: the permeability changed either enormously (three orders of magnitude) or only slightly (from no change to a quadrupling). The biggest change occurred in 30% of the shells. Importantly, the gas transport mechanism remained permeation, where the gas must dissolve in the plastic material, since heating the capsule to 300°C completely recovered the initial permeation and strength/modulus properties. The alternative gas transport mechanism is Knudsen diffusion, which would occur if pinholes or voids were created. These features would allow a gas/gas-surface diffusion process where gas can pass through a membrane without being absorbed into the material. This would be unacceptable since the shell would remain permeable at cryogenic temperatures, allowing the low-viscosity gas and liquid to easily pass out of the shell; as a result, the target would be unable to retain the deuterium fill.

When polymers are cooled, the activation energy for permeation increases and the permeability of the material decreases (more detail later in this article); however, an internal overpressure within the shell strains the wall and counteracts the decrease in permeability. This phenomenon was observed in 0.9-mm-diam plasma polymer shells filled with liquid deuterium (~51 μg) at 20 K (which equates to 1000-atm pressure at room temperature). When the shell was allowed to warm gradually, the internal pressure increased and the gas permeated out of the shell. Following this observation, the perme-
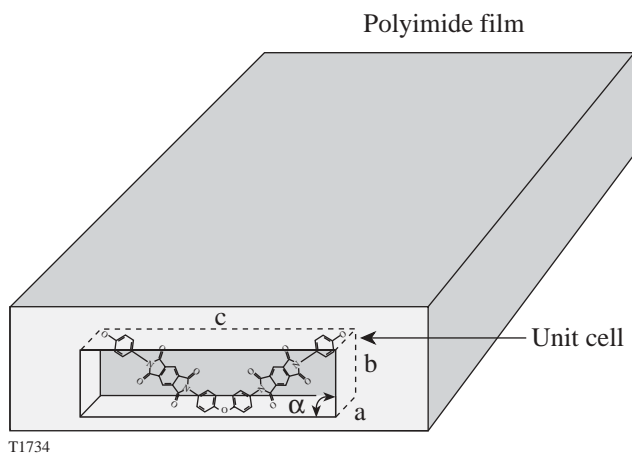
T1734

Figure 92.22
Schematic of the orientation of a polyimide crystal unit cell within the wall of a shell: $a = 6.31$ Å, $b = 3.97$ Å, $c = 32$ Å, and $\alpha = 90°$. The shaded planes of the unit cell represent the *00l* and *l00* lattice planes.

ation time constant for the shells at room temperature was measured and found to be unchanged. The only explanation for the shells not exploding when warmed gradually is that the permeability of the material changed as the shell expanded. By contrast, shells warmed rapidly explode as expected.

Once a thin-wall shell succumbs to an overpressure and bends, the intrinsic property of the material determines what happens next: brittle (plasma polymer, polystyrene) shells lack ductility and fracture into shards; polyimide, which is extremely elastic (typically tolerating up to 27% elongation), either collapses intact or tears apart, depending upon whether the overpressure is inside or outside the shell.

5. Surface Roughness of Polyimide Shells

Throughout this development program no effort has been made to optimize the smoothness of polyimide shells. This was considered a secondary priority, which would be addressed once the processing conditions and associated fundamental mechanical properties of the shell were accurately known.

Surface-roughness profiles of polyimide targets were acquired to establish a "typical" roughness power spectrum. Typically the roughness ranged from 0.5 to 1 μm with significant power throughout the spectrum. The low-order roughness was partially attributed to the quality of the mandrel on which the shell was formed; there had deliberately been no attempt to screen the quality of the mandrels for the smoothest and most-round ones because a large number of mandrels were required for the statistical study and the cost of analysis would have been prohibitive at that stage. The high-frequency roughness was corroborated with electron microscope images (Fig. 92.23) of the shells that showed "bumps" on the surface with lateral dimensions of 2 to 8 μm.
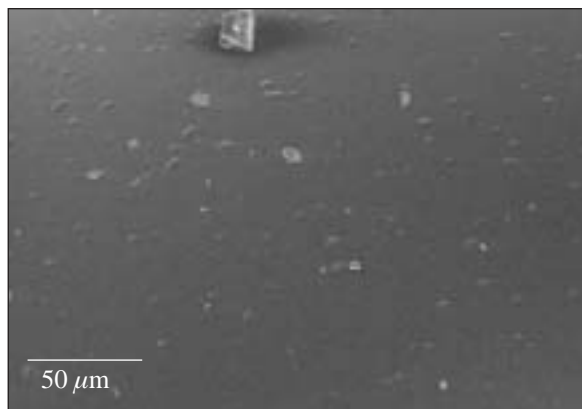
Issues Regarding Shells Specific to Processing Cryogenic Targets

1. Permeating Gas into Shells

The permeation coefficient (P) is the product of the diffusion coefficient (D) for a gas through a material and the solubility coefficient (S) of the gas in the material, where

$$P = S \times D = \left(\text{quantity of permeant}\right)$$

$$\times \left(\text{wall thickness}\right)/\left[\left(\text{area}\right)\times\left(\text{time}\right)\right.$$

$$\times \left(\text{pressure drop across shell}\right)\left.\right]. \qquad (3)$$

(The diffusivity has dimensions of area/time, and solubility has dimensions of molar-volume/pressure.)

The permeation time constant is an empirical figure of merit measured for all ICF capsules; it is the time required for 63% of the gas inside the shell to permeate out of the shell. This value depends on the wall thickness and the surface area and is independent of the pressure differential across the shell. Combining the time constant with the allowable buckling-pressure differential [Eq. (1)] gives the maximum rate at which a shell can be filled:

$$\text{Fill rate}\left(\text{atm/s}\right)$$

$$= \left(\text{buckling}\times\text{pressure}\right)/\left(\text{permeation}\times\text{time}\times\text{constant}\right).$$

Figure 92.23
Scanning electron micrograph of the surface of a 5-μm-wall PMDA-ODA shell. The overall surface is moderately smooth with the lateral dimensions of "bumps" below 10 μm. The larger particulates that are visible on the surface but removable are a consequence of the targets not being handled exclusively in a clean-room environment.

50 μm

T1718a

Direct-drive targets for experiments on the National Ignition Facility (NIF) are scaled versions of OMEGA targets and possess the same theoretical buckle pressures and time constants, so both types of shells can be filled at comparable rates. (Practically, larger-diameter targets are less spherical than smaller targets so the effective buckling pressure is marginally lower than would be expected by scaling smaller shells.) The larger diameter of a NIF target and the 350-μm-thick ice layer, however, will require 15 times more gas than an OMEGA target to achieve a scaled-thickness ice layer. A 100-μm ice layer for OMEGA targets requires approximately 1000 atm of gas at room temperature. (A 0.95-mm-diam shell at 295 K requires a fill pressure of 1027 atm to yield a 100-μm ice layer.) Filling targets at higher temperatures requires a higher pressure (1296 atm at 100°C for a 0.95-mm shell) since the gas density decreases with increasing temperature.

2. Effect of Temperature on the Permeability

Increasing the temperature not only increases the permeation rate but also decreases the elastic modulus (see Fig. 92.21), albeit less significantly, making permeation at elevated temperatures desirable. Table 92.II lists the time required to fill OMEGA and NIF direct-drive targets by permeation using different shell materials and different temperatures. Clearly, there is a major time benefit if shells can be filled at the maximum allowable temperatures. The maximum allowable temperature for the polyimide target is 400°C, which would require a fill pressure of 2210 atm, and the fill time would be reduced from 300 h to less than 10 h.

The temperature dependency of the permeability coefficient is given by

$$P = P_0 \exp\left(-E_p/RT\right),$$

where P_0 is the pre-exponential value [7×10^{-28} mol m/(m s Pa) for polyimide] and E_p (16.9 to 20.3 kJ/mol, depending upon the processing conditions) is the activation energy for permeation. The temperature dependency of the permeability of polyimide shells is reported from 130 K to 300 K[8,9] (Fig. 92.24) and for polyimide film to 523 K.[11]

3. Effect of Crystallinity on Permeability

The permeability of polyimide varies moderately according to the processing conditions and is affected by the crystallinity of the material. Permeation proceeds through a mechanism that requires polymeric chains to move over a very localized area to accommodate the movement of dissolved gas molecules through the plastic; this is referred to as the "segmental

Table 92.II: Calculated minimum time required to fill targets by permeation. The targets are (1) a 0.95-mm-diam shell with a 1-μm wall and a 100-μm ice layer for cryogenic experiments on OMEGA; and (2) a 3.4-mm-diam shell with a 3-μm wall and a 350-μm ice layer for cryogenic experiments on the NIF. Different permeation temperatures are presented where the mechanical and permeation properties are known. The ^{3}He density increases at a rate of 0.02 mg/cm^3/day.

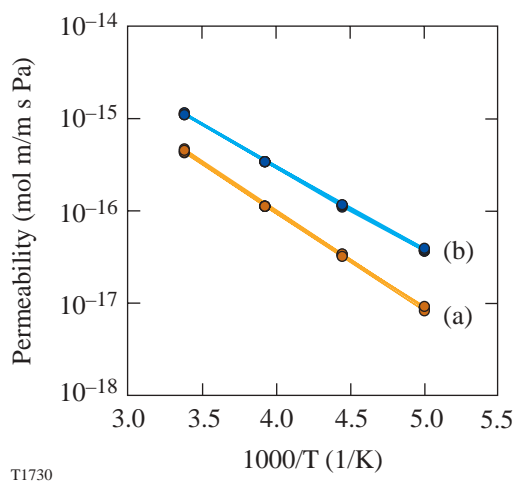| Target	Permeation Time Constant (s)	Required Fill Pressure (atm)	Fill Time (h)
Plasma polymer at 295 K (OMEGA)	10	1027	25.4
Plasma polymer at 373 K (OMEGA)	2.7	1296	8.5
Plasma polymer at 295 K (NIF)	106.8	101	375
Plasma polymer at 373 K (NIF)	28.5	1263	126
Polyimide (PMDA-ODA formulation) at 295 K (OMEGA)	184	1027	320
Polyimide (PMDA-ODA formulation) at 573 K (OMEGA)	1.8	1925	10.2

T1730

Figure 92.24
The temperature-dependent helium permeability of polyimide processed in nitrogen (a) is lower than when it is processed in air (b) due to the increased crystallinity and stiffness of the polymer.
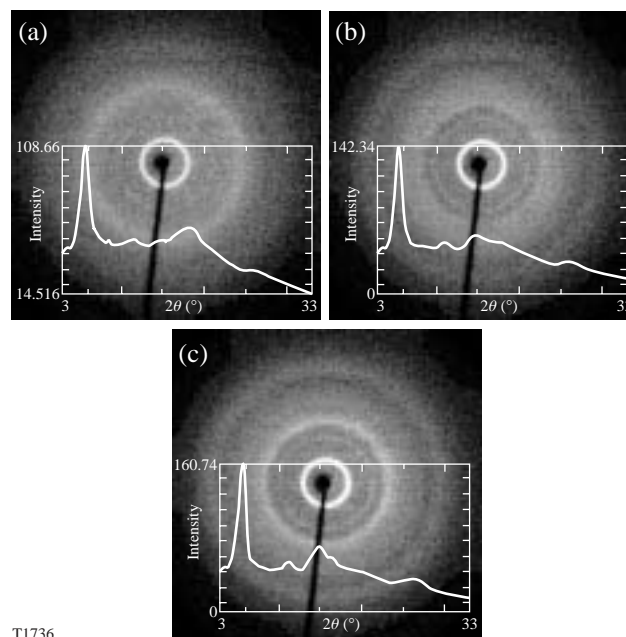

T1736

Figure 92.25
Comparison of transmission-mode x-ray diffraction patterns of polyimide shells imidized at increasing rates (a) 0.1 C/min, (b) 1 C/min, and (c) 5 C/min, together with integrated 2θ plots. The increased intensity of the *002* peaks at 5.7°. 2θ indicated greater crystallinity and is associated with lower permeability.

mobility" of the polymer. Amorphous material predictably is more permeable than crystalline material since the crystallinity increases the rigidity of the polymer chain. Another consideration is the scale length of the crystal: materials with similar overall crystallinity are more permeable if the crystalline regions are larger and more sparsely distributed than if there is a greater number of smaller, more-distributed regions—a channeling effect.[8,9]

The effect of changing an important processing variable—the imidization rate—is to change the size and distribution of crystals without changing the overall degree of crystallinity. Polyimide shells that are formed using a rapid imidization process (5 C/min) show more-intense, narrower 002 x-ray diffraction peaks than do polyimide shells that are made using a gradual imidization rate (0.1 C/min) (Fig. 92.25). The peaks of the rapidly imidized material are better aligned in the plane of the shell, as shown by grazing-angle x-ray diffraction data.[8,9] Finally, the material that was rapidly imidized has larger-scale, better-oriented crystalline regions that are more dispersed throughout the amorphous material, and this morphology corresponds to a more-permeable material.

By changing a second processing condition and imidizing polyimide shells in an air rather than a nitrogen atmosphere, the degree of crystallinity was reduced and the permeability of the material increased by 20%.

4. Effect of Mechanical Strain on the Permeability

Stressing polyimide beyond the yield stress—80 MPa at 3% strain—plastically deforms the material. (The ultimate yield stress of the vapor-deposited polyimide is 280 MPa at a biaxial strain of 27%.) As the polyimide shell is cooled inside the Cryogenic Target Handling System's (CTHS's) permeation pressure vessel, it is strained; the tensile and compressive nature of the strain varies over the entire temperature range as a complex function of the properties of the gas and materials at different temperatures. Given the exceptionally low buckling strength of the shell compared to the burst strength, it is desirable to maintain the shell in a regime where there is a net tensile (burst) force. This increases the risk that the stress may exceed the yield stress and the polyimide wall will be plastically deformed. The diameter of the shell will then increase, and the thickness of the ice layer will decrease proportionally, adding uncertainty to the dimensions of the target when it is shot. A maximum strain limit of 3% in the shell is the recommended design point for establishing the thermal performance of the permeation cell. Temperature gradients within the permeation cell, during either steady state or unsteady state, that translate into pressure gradients exceeding the 3% limit across the shell wall are unacceptable.

A consequence of biaxially straining polyimide shells beyond a 15% level is a change in the permeability of the material. As described above, approximately 1/3 of all shells strained to this level have an ~1000-fold increase in permeability. There are two intriguing aspects to this behavior: first, that the increased permeability is so sizeable, and second, that the behavior is stochastic. An explanation for this behavior is that strain introduces a microstructural change to the material. Supporting evidence is that the elastic modulus (stiffness) decreases by 56% (to 1.5 GPa) when strained and the crystallinity decreases substantially (see Fig. 92.26).[5,9,10] It is presumed that the statistical nature to the change in magnitude of the permeability is in the random initial distribution of crystalline and amorphous phases in the material, and the response of the material to the strain. Doubtlessly, strain changes the morphology; however, permeation will increase only if there is a contiguous alignment of highly mobile polymer chains through the shell wall—and this eventuality is statistical. Very important for confirming that this phenomenon is a microstructural event is the observation that the original elastic modulus and permeability values are returned when a strained and highly permeable shell is heated to 300°C. At the high temperature the plastic becomes more fluid and the strain-induced morphological change is reversed.
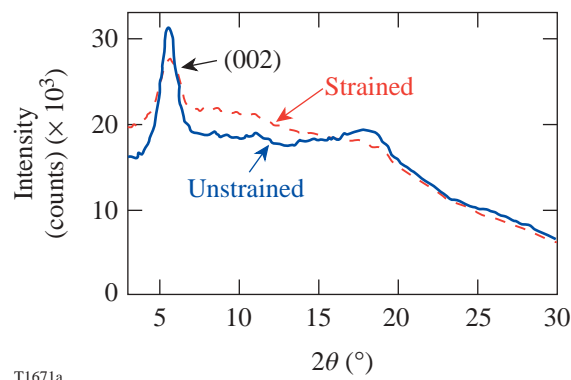

T1671a

Figure 92.26
Comparison of transmission-mode x-ray diffraction patterns of polyimide shells for unstrained and mechanically biaxially strained polyimide shells showing appreciably greater crystallinity present in the unstrained shell.

5. Effect of Chemical Modification to the Polyimide on the Permeability

An alternative way to modify the segmental mobility of the polymer chain to enhance the permeability is to add flexible chemical units into the backbone of the polymer. Figures 92.19 and 92.27 compare the chemical formulation of two vapor-deposited polyimide shells: (a) the original PMDA-ODA–based polyimide discussed in detail here and (b) a 6FDA-ODA formulation that adds a flexible fluorine-based linkage to the polymer chain, respectively.[13,14]
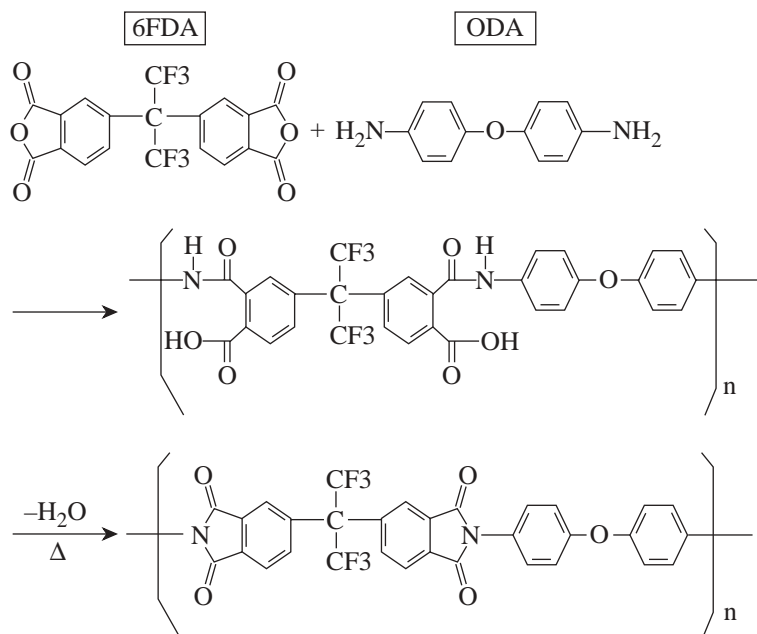

T1716

Figure 92.27
Structural and elemental composition of a permeable fluorinated-polyimide formulation.

The disadvantage of using the fluorinated polyimide for ICF experiments is the presence of fluorine (10 at. %) and the consequent x-ray preheat that will occur during an implosion. The advantages are numerous: The deuterium permeability is 50× greater than traditional PMDA-ODA–based polyimide, while the elastic modulus is only 18% lower. This reduces the time required to fill the shell with 1000 atm of deuterium at room temperature from 333 h to 8.8 h. (Note that this compares the fluorinated polyimide against the nonmechanically strained PMDA-ODA polyimide.)

The second advantage of using the polyimide based on 6FDA-ODA chemistry is the lower activation energy from permeation compared to polyimide made using PMDA-ODA chemistry, 12.3 versus 20.1 kJ/mol[12] (see Fig. 92.28). This will allow the fluorinated polyimide to retain higher permeability as the capsule is cooled (discussed in detail in the next section) to alleviate pressure differentials across the shell due to temperature gradients within the permeation pressure vessel.

6. Evaluation of Different Treatment Processes on the Processing Time Required to Fill Cryogenic Targets by Permeation

The critical parameters and the associated time required to fill OMEGA- and NIF-scale cryogenic shells are listed in Table 92.III for four different types of shells: (1) a standard plasma polymer shell, (2) a standard polyimide shell, (3) a
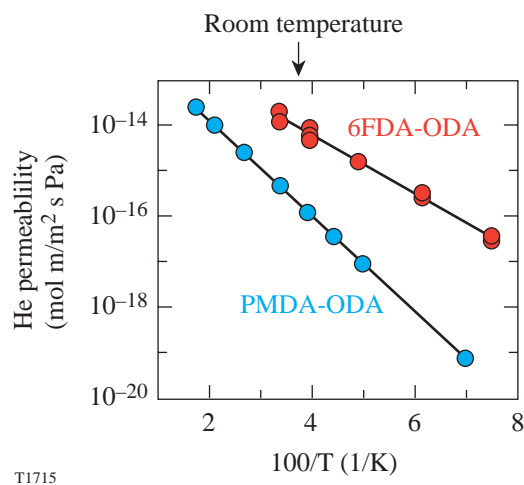

Figure 92.28
Arrhenius plot comparing the permeability of polyimide formulations: PMDA-ODA and 6FDA-ODA, over a wide temperature range.

polyimide shell structurally modified to enhance the permeability, and (4) a polyimide shell chemically modified to enhance the permeability. There is a clear time advantage, from a processing perspective, to using the more recently developed mechanically and chemically modified polyimide shells; however, these shells have other disadvantages when considering the processability of the target or the implosion performance of the target.

Table 92.III: Calculated minimum time to fill by permeation three different types of polyimide shells and a plasma polymer shell for OMEGA and the NIF. Target dimensions, respectively, are 0.95-mm-diam, 1.0-μm wall and 100-μm ice layer; and 3.5-mm-diam, 3.0-μm wall and 350-μm ice layer. The temperature is 295 K.

Polyimide Material	Fill Time (h) (OMEGA)	Fill Time (h) (NIF)
Baseline polyimide (PMDA-ODA formulation)	320	205 days
Mechanically strained polyimide (PMDA-ODA formulation)	0.66	21
Fluorinated polyimide (6FDA-ODA formulation)	8.0	121
High-density CH plasma polymer	25.4	375

Cooling Targets

Once the permeation cycle is complete, the pressure inside the shell is equal to the pressure outside the shell. The entire pressure vessel is then cooled to 26 K. During this process the vessel must be cooled uniformly to minimize the pressure gradient that develops across the shell. Inevitably a thermal gradient will develop along the internal perimeter of the permeation pressure vessel and also between the perimeter and the center where the shell is located. This is the most-precarious phase for the survival of the target: while transient temperature gradients during cooling do not induce pressure gradients within the gas on the time scale of interest, a pressure gradient does develop across the shell wall.

The ideal shell material would be one with the highest-possible stiffness, strength, and yield strength (in both compression and tension) to resist the pressure difference, and the highest-possible permeability over the widest temperature range down to 30 K to alleviate the pressure differential. Finally, permeation must be negligible at 26 K, the temperature where the liquid/gaseous deuterium outside the shell is removed, leaving a shell containing 51 μg of liquid deuterium with a vapor pressure of ~2 atm. One last desirable property is that the material resists damage from electron radiation when tritium gas is used.

At the beginning of the cooling cycle, at temperatures where polyimide is still permeable, any pressure gradient is minimized by permeation. As the temperature decreases, the permeability of the shell also decreases. At lower temperatures, slower cooling rates are required to allow longer periods for the pressure gradient across the shell to be reduced. When the shell becomes impermeable, the survival of the shell depends on whether any further thermally induced pressure gradient exceeds the shell's buckle or burst strengths. If the thermally induced pressure gradients remain too high, the only remedy is to improve the thermal uniformity of the permeation pressure vessel.

Thermal modeling of the permeation cell in the OMEGA CTHS reveals that a 1-K temperature change at the perimeter induces a 0.5-atm pressure differential across the shell wall at 295 K and a 0.9-atm pressure differential at 60 K. At these densities the thermal diffusivity is moderately low, and the thermal time constant is ~30 s. This pressure differential creates a bursting force since the perimeter of the permeation vessel is colder and hence denser than the center of the vessel where the shell is located. This load is in addition to other phenomena such as the thermally induced contraction of the shell (which generates a net bursting pressure) and the temperature of the gas in the plumbing that connects the permeation vessel to a valve at room temperature (which creates a net buckling pressure). Depending on the cooling rate, the thermal uniformity of the permeation cell, and the temperature-dependent permeability of the polyimide, the shell can pass from a buckle to burst regime and back as the temperature decreases.

The weakest failure mode for shells is buckling, and the buckling strength of a thin-wall polyimide shell (nominal 1-μm wall) is 0.13 atm. The burst strength for a 1-μm wall shell is ~4 atm, whereas the yield strength is ~1 atm. A practical constraint in the design of the equipment is the accuracy of the silicon diode temperature sensor used to regulate the temperature ramp: in practice, the accuracy is ±0.5 K at 300 K. This value, the long thermal time constant for the permeation vessel, and the shorter thermal time constant for the gas to respond to temperature gradients combine to limit the value of using active temperature control over the temperature environment to minimize the likelihood of bursting/buckling the shell. Clearly the thermal environment within the pressure vessel has to be engineered to remain as constant as possible over a wide temperature and pressure range: from 18 K to 573 K and 1000 atm to a maximum of 2200 atm (33,000 psi), respectively.

The OMEGA Cryogenic Target Handling System has demonstrated that it is possible to process 0.95-mm-diam shells with walls as thin as 2.5 μm at room temperature over a period of three days. With the design goal being to process a 0.95-mm-diam shell with a 1-μm wall in less than two days, advanced shell materials and improved thermal engineering of the equipment are required. Greater strength will provide greater margin for the design of the permeation cell and will also offset possible strength degradation from radiation damage.

The future use of tritium adds two complications to the process: (a) hydrogen embrittles many metals, limiting the selection of available alloys for making the pressure vessel, and (b) the potential radioactive hazard requires heightened safeguards.

Radiation Effects

The decay of a triton produces an electron with a mean energy of 6 keV and an energy range of 2 to 18 keV.[6] The effect of this electron on a polymer is to rupture chemical bonds and weaken the material.[6] Given the high DT density in a target (0.11 gm/cm^3 for pressurized gas and 0.25 gm/cm^3 for ice), the stopping power of the medium is appreciable and the 1/e

penetration distance is less than 30 μm. Consequently, only tritium dissolved in the plastic wall and the tritium immediately adjacent to the plastic wall damage the plastic.

During the processing of cryogenic targets there are three phases where tritium decay is an issue: (1) during the pressure ramp, (2) during the cooling cycle, and (3) during layering. During the pressure ramp (0.05 atm/min for a 1-μm-wall shell) the dose from the tritium dissolved in the wall (assuming 10% solubility at 1 atm scales linearly with increasing pressure) will be approximately 50 MGy. Added to this is the contribution from tritium adjacent to the shell wall, which is less than 2 MGy. During cooling at a rate of 0.1 K/min, the dose will be 6 MGy, the majority coming from gas dissolved in the plastic and less than 1 MGy from the adjacent gas volume. When ice has formed and layered, the dose, primarily from the adjacent ice layer, will be 0.3 MGy/h. This contribution is smaller since the 1/e penetration distance is only 9 μm at ice density and the amount of tritium dissolved in the wall is negligible. Allowing 36 h to layer and deliver a target, the total dose to the shell material may be expected to be of the order of 70 MGy. These radiation doses are estimates based on the penetration distance of 6-keV electrons at discrete temperatures and densities. A rigorous analysis would be considerably more complex and require more-detailed information than is available. The purpose of this analysis was to estimate the dosage for subsequent radiation-induced damage experiments.

In an effort to quantify the effect that radiation damage from tritium decay may have on polyimide, polyimide shells were irradiated with an electron beam from a scanning electron microscope. The electron energy was 8 keV, and the current flux calculated to be 7 mA/m^2. The total integrated dose was 60 and 120 MGy. The results are summarized as follows: the elastic modulus showed no change with exposure; the tensile strength decreased from 280 MPa (initially) to 266 MPa at the 60-MGy dose and 240 MPa at the 120-MGy dose; and the permeability did not change with dose. The property that showed the biggest change was the elasticity/plasticity of the system: the maximum elongation that polyimide can withstand is 27%. Exposure to 60 MGy reduces this to 20%, and exposure to an additional 60 MGy further reduces this to 14%. None of these performances will impair polyimide sufficiently to affect the likely survivability of the shell, but two important issues remain: any impairment to the yield strain was not determined, and any change in the transparency of the material was not investigated.

The observed radiation resistance is an important consideration when evaluating polyimide material as a potential shell material. Literature values for the performance of polystyrene (which possesses a chemical composition similar to plasma polymer) suggest that the mechanical properties are considerably more impaired than for heavily conjugated organic structures such as polyimide.[6]

Conclusions

Polyimide shells suitable for ICF cryogenic experiments on OMEGA were developed, and the associated mechanical properties were determined to define the processing conditions for operating the OMEGA Cryogenic Target Handling System. Overall, polyimide targets offer a viable alternative to plasma polymer capsules currently in use. The greatest virtue for the polyimide material is its high radiation resistance (for tritium application) and its excellent mechanical properties, which lessen the demanding specifications for the equipment needed to provide cryogenic targets.

The single biggest limitation to using the most thoroughly developed and characterized polyimide, based on PMDA-ODA chemistry, is the low permeability of the material at room temperature. This increases the processing time and exacerbates the deleterious effect of ^{3}He production on the performance of the implosion. Importantly, there are solutions to this problem, but each has its own implications: (1) The permeation time can be reduced substantially by filling shells at elevated temperature (up to 300°C), but this adds to the complexity of the cryogenic system needed to provide these targets. (2) The permeability can be dramatically increased by mechanically straining polyimide to modify the crystalline microstructure of polyimide, which achieves the shortest-possible fill time. The technique has not been thoroughly developed, however, and cannot yet be relied upon for routine production: the yield is low and the magnitude and effect of the shell deformation during the process remain too variable and not fully determined. The production aspects for this process have to be developed further. (3) The final option for increasing the permeability of polyimide is the most promising: change the chemical formulation to add flexibility to the polymer chain. Not only does this increase the permeability at room temperature, but it also increases the permeability of the material over a broad temperature range—a property that will increase the survivability of thin-wall targets during processing. The disadvantage of this approach is the presence of fluorine in the polymer and the effect fluorine has on the implosion physics.

REFERENCES

1. S. A. Letts *et al.*, Fusion Technol. **28**, 1797 (1995).

2. J. J. Sanchez and S. A. Letts, Fusion Technol. **31**, 491 (1997).

3. E. L. Alfonso, S. H. Chen, R. Q. Gram, and D. R. Harding, J. Mater. Res. **13**, 2988 (1998).

4. F.-Y. Tsai, E. L. Alfonso, S. H. Chen, and D. R. Harding, Fusion Technol. **38**, 83 (2000).

5. F.-Y. Tsai, D. R. Harding, S. H. Chen, T. N. Blanton, and E. L. Alfonso, Fusion Sci. Technol. **41**, 178 (2002).

6. *Safe Handling of Tritium: Review of Data and Experience*, Technical Reports Series No. 324 (IAEA, Vienna, 1991).

7. E. H. Baker, L. Kovalevsky, and F. L. Rish, *Structural Analysis of Shells* (McGraw-Hill, New York, 1972).

8. F.-Y. Tsai, T. N. Blanton, D. R. Harding, and S. H. Chen, "Temperature Dependency of the Properties of Vapor-Deposited Polyimide," to be published in the Journal of Applied Physics.

9. F.-Y. Tsai, "Engineering Vapor-Deposited Polyimides," Ph.D. thesis, University of Rochester, 2002.

10. F.-Y. Tsai, E. L. Alfonso, D. R. Harding, and S. H. Chen, J. Phys. D: Appl. Phys. **34**, 3011 (2001).

11. *Polyimides: Fundamentals and Applications*, edited by M. K. Ghosh and K. L. Mittal, Plastics Engineering, Vol. 36 (Marcel Dekker, New York, 1996).

12. Laboratory for Laser Energetics LLE Review **81**, 6 and 21, NTIS document No. DOE/SF/19460-335 (1999). Copies may be obtained from the National Technical Information Service, Springfield, VA 22161.

13. A. Nikroo, General Atomics, private communication (2002).

14. F.-Y. Tsai, D. R. Harding, S. H. Chen, and T. N. Blanton, "High-Permeability Fluorinated Polyimide Microcapsules by Vapor-Deposition Polymerization," to be published in Polymer.